Experimental Realization of a 2D Fractional Quantum Spin Liquid

R. Coldea,[1,2] D. A. Tennant,[2,3] A. M. Tsvelik,[4] and Z. Tylczynski[5]

[1]*Oak Ridge National Laboratory, Oak Ridge, Tennessee 37831*
[2]*ISIS Facility, Rutherford Appleton Laboratory, Chilton, Didcot, Oxon OX11 0QX, United Kingdom*
[3]*Oxford Physics, Clarendon Laboratory, Parks Road, Oxford OX1 3PU, United Kingdom*
[4]*University of Oxford, Department of Theoretical Physics, 1 Keble Road, Oxford OX1 3NP, United Kingdom*
[5]*Institute of Physics, Adam Mickiewicz University, Umultowska 85, 61-614 Poznan, Poland*
(Received 11 July 2000)

The ground-state ordering and dynamics of the two-dimensional $S = 1/2$ frustrated Heisenberg antiferromagnet Cs_2CuCl_4 are explored using neutron scattering in high magnetic fields. We find that the dynamic correlations show a highly dispersive continuum of excited states, characteristic of the resonating valence bond state, arising from pairs of $S = 1/2$ spinons. Quantum renormalization factors for the excitation energies (1.65) and incommensuration (0.56) are large.

DOI: 10.1103/PhysRevLett.86.1335 PACS numbers: 75.10.Jm, 05.30.Pr, 75.40.Gb

The concept of fractional quantum states is central to the modern theory of strongly correlated systems. In magnetism, the most famous example is the spin $S = 1/2$ 1D Heisenberg antiferromagnetic chain (HAFC), where pairs of $S = 1/2$ spinons are deconfined from locally allowed $S = 1$ states; a phenomenon that is now well established both theoretically [1] and experimentally [2]. These spinons are topological excitations identified with quantum domain walls. Experimentally, such fractionalization is manifest as a highly dispersive continuum in the dynamical magnetic susceptibility measured by, e.g., neutron scattering [2], and for the HAFC identified as the creation of pairs of spinons.

In 1973, Anderson [3] suggested that a 2D fractional quantum spin liquid may take the form of a "resonating valence bond" (RVB) state comprising singlet spin pairings in the ground state, and with pairs of excited $S = 1/2$ spinons separating via rearrangement of those bonds. The dominant feature of the RVB state, present in all its theoretical descriptions [4–6], is an extended, highly dispersive, continuum. To date this feature remains unobserved in any 2D magnet; in the case of the $S = 1/2$ Heisenberg square lattice (HSL) mean-field confining effects lead to $S = 1$ magnons and a renormalized classical picture of fluctuations around local Néel order emerges [7,8]. One may think, however, that because frustrating interactions can counteract the staggered fields responsible for confinement [8,9] they may provide a route to generating fractional phases in 2D.

We explore such a scenario by making neutron scattering studies on Cs_2CuCl_4. By exploiting its unique experimental properties as a low-exchange quantum magnet [10], we reveal an unexpectedly strong two dimensionality in the form of a triangular antiferromagnet with partially released frustration. The simplicity of the couplings in Cs_2CuCl_4 makes it a model system to investigate generic features of 2D frustrated quantum antiferromagnets.

The structure of Cs_2CuCl_4 is orthorhombic (*Pnma*) with lattice parameters $a = 9.65$ Å, $b = 7.48$ Å, and $c = 12.35$ Å at 0.3 K. Magnetic interactions are mostly restricted between Cu^{2+} $S = 1/2$ spin sites in the (b, c) plane [see Fig. 1(a)] with coupling J along b ("chains") and zigzag "interchain" coupling J' along the c axis [11]. A small interlayer coupling $J'' < 10^{-2}J$ (along a) stabilizes 3D order below $T_N = 0.62$ K into an

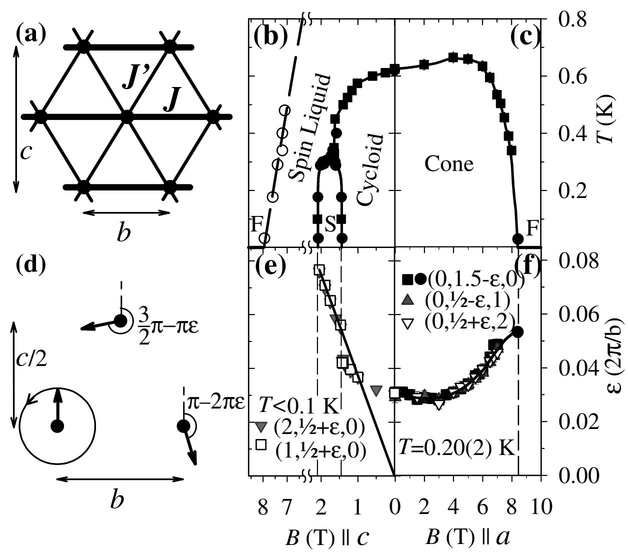

FIG. 1. (a) 2D couplings in Cs_2CuCl_4: Strong bonds J (thick lines) and smaller frustrating zigzag bonds J' (thin lines). (b),(c) Magnetic phase diagram in a field along the c and a axes, respectively. Symbols show the boundaries of the various phases described in the text, measured using neutron scattering (squares) [11,13] and susceptibility (circles) [13]. Solid curves are a guide to the eye, and the dashed line indicates crossover to paramagnetic behavior. (d) Spin rotation in the (b, c) plane. Thick arrows are spin vectors, and the circle indicates the spin rotation upon translation along the b axis. (e) Incommensuration ϵ vs field along c [13]. (f) ϵ vs field along a (solid line is a guide to the eye, and the solid circle is from [13]).

incommensurate structure along b due to the frustrated couplings; weak anisotropies confine the ordered moments to rotate in cycloids near coincident with the (b, c) plane [see Fig. 1(d)] but with a small tilt of the cycloidal plane relative to the (b, c) plane whose sense alternates along c such that for each plaquette (isosceles triangle) $\langle \mathbf{S}_1 \cdot (\mathbf{S}_2 \times \mathbf{S}_3) \rangle$ is small but nonzero (order is noncoplanar) [11], making this system a candidate for a chiral spin state [12]. The minimal Hamiltonian determining the magnetic order is

$$\mathcal{H} = \sum_{\langle i,i' \rangle} J\mathbf{S}_i \cdot \mathbf{S}_{i'} + J' \sum_{\langle i,j \rangle} \mathbf{S}_i \cdot \mathbf{S}_j \qquad (1)$$

with each interacting spin pair counted once [see Fig. 1(a)]; a detailed description of the full Hamiltonian including small Dzyaloshinskii-Moriya terms is given elsewhere [13]. The Hamiltonian interpolates between noninteracting HAFCs ($J' = 0$), the fully frustrated triangular lattice ($J' = J$), and unfrustrated HSL ($J = 0$).

Quantifying the couplings in (1) is of considerable importance both to guide theory and put our results in context. We do this using the following approach: neutron diffraction measurements were made on a single crystal of Cs_2CuCl_4 in magnetic fields up to 7 T and temperatures down to 0.2 K using the PRISMA time-of-flight (TOF) spectrometer at the ISIS spallation neutron source. For fields along a (near perpendicular to the planes of spin rotation) a 3D incommensurate "cone" order is stable up to full ferromagnetic (F) alignment ($B_c = 8.44$ T at $T = 0.03$ K) [see Fig. 1(c)]. At $T = 0.2$ K magnetic Bragg peaks arising from the *transverse* spin rotation move from $\epsilon_0 = 0.030(2)$ in zero field to $\epsilon = 0.047(2)$ at 7 T, where ϵ is the incommensuration relative to Néel order [see Fig. 1(f)]. Mean-field theory predicts no change with field, and the large renormalization observed is a purely quantum effect. Since the ferromagnetic (F) state is an eigenstate of (1) with no fluctuations, ϵ at the saturation field B_c is at its classical value [14] $\sin \pi \epsilon_c = J'/2J$. Higher-field measurements [13] observe $\epsilon_c = 0.053(1)$, implying an exchange coupling ratio of $J'/J = 0.33(1)$. The resulting quantum renormalization of the zero-field incommensuration $\epsilon_0/\epsilon_c = 0.56(2)$ is similar to the predicted value of 0.43(1) [$J'/J = 0.33(1)$] estimated by series expansions using a paired singlet basis [14]. Additionally, the determined exchange coupling ratio is in agreement with the observed 2D dispersion in the saturated phase at 12 T $\parallel a$ [13], which give the bare exchange couplings-per-site $J = 0.375(5)$ meV within chains and $2J' = 0.25(1)$ meV between chains. *This demonstrates that interchain couplings are of the same order as "intrachain" and Cs_2CuCl_4 is therefore a quasi-2D system.* These observations require a change in the point of view taken by earlier studies [10], which proposed a quasi-1D picture based on estimates of the interchain couplings, not including the large quantum renormalization of the incommensuration reported here. We now present detailed measurements of the excited states.

Dynamical correlations in a 2.5 cm^3 single crystal of Cs_2CuCl_4 were probed using the indirect-geometry TOF spectrometer IRIS, also at ISIS. The energy resolution [0.016 meV full width at half maximum (FWHM)] was an improvement of nearly an order of magnitude compared to our previous studies [10]. The detectors form a semicircular 51-element array covering a wide range of scattering angles (25.75° to 158.0°). The sample was mounted with the (a, b) scattering plane horizontal in a dilution refrigerator insert with base temperature 0.1 K.

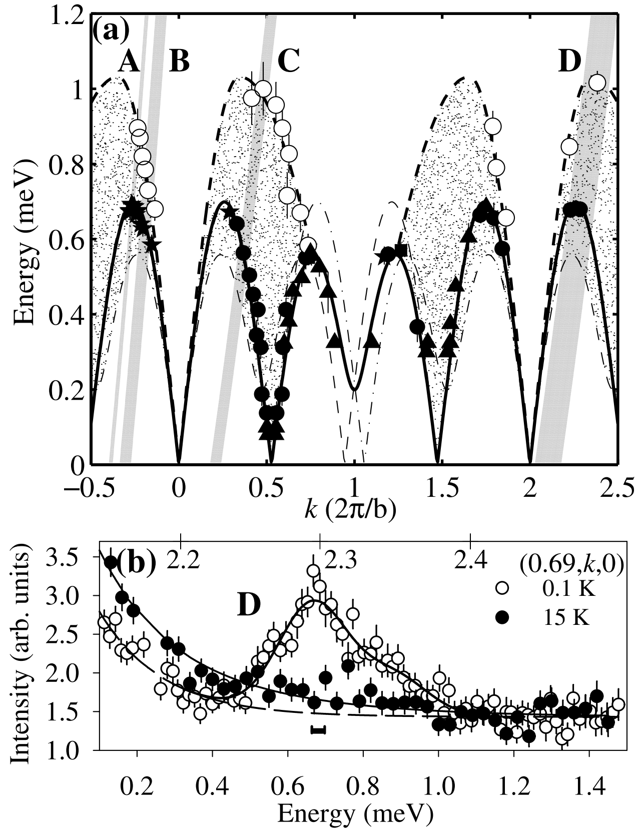

FIG. 2. (a) Dispersion of the magnetic excitations along the b^* axis ($T = 0.1$ K, zero field). Filled symbols (triangles from [10]) show the main peak in the measured line shape and the solid line is a fit to the principal spin-wave mode $\omega(k)$ of Hamiltonian (1) (dashed and dash-dotted lines show the corresponding dispersion of the other two secondary modes, ω^+ and ω^-, respectively, as described in the text). Typical scan trajectories are shown by the light shaded regions labeled *A-D* (the line thickness is the wave-vector averaging) and the measured data are shown in Figs. 3(A)–3(D). The open circles show the experimentally estimated upper boundary of the continuum and the upper (thick) dashed line is a guide to the eye. The dotted area indicates the extent of magnetic scattering. (b) Intensity measured along scan D above, in the cycloidal phase at 0.1 K (open circles) and in the paramagnetic phase at 15 K (solid circles). Data points are the raw counts and the dashed line shows the estimated nonmagnetic background. The solid lines are guides to the eye and the horizontal bar indicates the instrumental energy resolution.

The results for the $\mathbf{b}^*$ dispersion are shown in Fig. 2(a). Although the data points also have a finite wave-vector component along $\mathbf{a}^*$, no measurable dispersion could be detected along this direction, confirming that the coupling between layers J'' is negligible. The observed dispersion is well accounted for by the principal spin-wave mode [15] of Hamiltonian (1), $\omega(\mathbf{k}) = \sqrt{(J_{\mathbf{k}} - J_{\mathbf{Q}})\,[(J_{\mathbf{k-Q}} + J_{\mathbf{k+Q}})/2 - J_{\mathbf{Q}}]}$, where the Fourier transform of exchange couplings is $J_{\mathbf{k}} = \tilde{J}\cos 2\pi k + 2\tilde{J}'\cos\pi k\cos\pi l$ and $\mathbf{k} = (h,k,l)$. The ordering wave vector in the 2D Brillouin zone of the triangular lattice is $\mathbf{Q} = (0.5 + \epsilon_0)\mathbf{b}^*$ and the effective exchange parameters $\tilde{J} = 0.62(1)$ meV and $\tilde{J}' = 2\tilde{J}\sin\pi\epsilon_0$ (fixed) are in agreement with [10]. The quantum renormalization of the excitation energy $\tilde{J}/J = 1.65$ is very large and is similar to the exact result $\pi/2$ for the 1D $S = 1/2$ HAFC (see, e.g., [1]). In contrast, the spin-wave velocity (energy) renormalization in the unfrustrated $S = 1/2$ HSL is only 1.18. *Such large renormalizations of energy (1.65) and incommensuration (0.56) show the crucial importance of quantum fluctuations in the low-field state of* Cs_2CuCl_4.

A remarkable feature of the measured dynamical correlations is that these do not show single particle poles, but rather extended continua. Figure 2(b) (open circles) shows a scan at the magnetic zone boundary taken at 0.1 K. The scattering is highly asymmetric with a significant high-energy tail. The nonmagnetic background (dashed line) is modeled by a constant-plus-exponential function. The magnetic peak disappears at 15 K (solid circles) and is replaced by a broad, overdamped, paramagnetic signal. Figures 3(A)–3(D) show 0.1 K data properly normalized and corrected for absorption, and with the nonmagnetic background subtracted. To quantify discussion of the dynamical correlations measured by neutron scattering, we first consider a spin-wave model, which is known to provide a good description of the unfrustrated HSL [7].

The dynamical correlations of the spin-wave model [15] for Hamiltonian (1) exhibit single particle poles from three spin-1 magnon modes, polarized with respect to the cycloidal plane. Figure 2(a) shows the main dispersion mode $\omega(k)$, polarized out of plane, and the two secondary modes, $\omega^-(k) = \omega(k - Q)$ and $\omega^+(k) = \omega(k + Q)$, both polarized in plane, where the equilibrium spin direction rotates in plane with wave vector Q. The expected scattering is given by the dashed lines in Figs. 3(A)–3(D), which clearly fails to account for the observed intensity as well as the extended high-energy tail of the scattering. This tail is not an instrumental effect as the FWHM of the energy resolution [horizontal bar in Fig. 2(b)] is an order of magnitude narrower than the signal width. Including next-order processes also fails to account for the scattering: the two-magnon scattering (polarized in-plane) contribution to the line shape is also shown in Fig. 3(D) (shaded area)—this was calculated numerically using the method described in [16] and using the experimentally

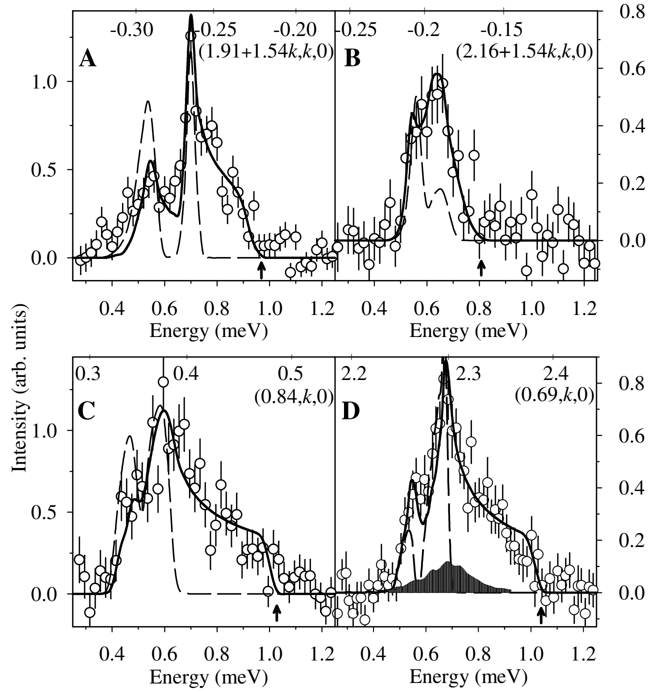

FIG. 3. Magnetic inelastic scattering measured at 0.1 K along the light shaded regions labeled *A-D* in Fig. 2(a). Top axis shows wave-vector change along scan direction. Counting times were typically 35 hours at an average proton current of 170 μA. Solid lines are fits to a modified two-spinon cross section (see text). Vertical arrows indicate estimated upper boundary. Dashed lines show predicted line shape for polarized cycloidal spin waves and the dark shaded region (shown only in *D* for brevity) indicates the estimated two-magnon scattering continuum. All calculations include the isotropic magnetic form factor of Cu^{++} ions and the convolution with the spectrometer resolution function.

estimated spin reduction $\Delta S \sim 0.13$ [11] to normalize the elastic, one- and two-magnon scattering.

Because in a neutron scattering process the total spin changes by $\Delta S_{\text{total}} = 0, \pm 1$, the absence of single particle poles and the presence of excitation continua imply that the underlying excitations carry fractional quantum numbers. For $J' = 0$, these are rigorously known to be $S = 1/2$ spinons [1], and two-spinon production is the principal neutron scattering process [2]. Our analysis shows that the measured scattering can be described by the Müller ansatz line shape appropriate to the 1D $J' = 0$ limit $S(k,\omega) \sim \Theta[\omega - \omega_l(k)]\Theta[\omega_u(k) - \omega]/\sqrt{\omega^2 - \omega_l^2(k)}$, where Θ is the Heaviside step function, and ω_l and ω_u are the lower and upper continuum boundaries, respectively, generalized to 2D such that (i) the total cross section has three continua with the lower boundaries $\omega(k)$, $\omega^-(k)$, and $\omega^+(k)$ shown in Fig. 2(a), (ii) the continua have equal weights and are isotropic in spin space, and (iii) a modified upper boundary ω_u [dashed upper line in Fig. 2(a)] is used. This model provides an excellent description of the data [see Figs. 3(A)–3(D)]. It is also noteworthy that both the asymmetric dispersion, characteristic of 2D frustrated couplings, and the excitation continua are essentially unchanged at $T = 0.9$ K above $T_N = 0.62$ K in the disordered spin liquid phase showing that ordering affects only the low-energy behavior. We conclude that, *in contrast to the HSL ($J = 0$) where unfrustrated couplings confine spinons into $S = 1$ magnons throughout the Brillouin zone, Cs_2CuCl_4 has fractional spin quasiparticles carrying the same quantum numbers as in the HAFC ($J' = 0$), namely, $S = 1/2$ spinons, and that, further, these spinons are modified by the two dimensionality at all energy scales*. Although no evidence of spinon confinement is observed at any of the energy scales probed in our experiments, low energy $S = 1$ Goldstone modes are expected to occur in the 3D ordered phase; weakly coupled HAFCs have recently been shown to exhibit dimensional crossover in the dynamical correlations from low-energy 3D spin waves to high-energy 1D spinon continua on an energy scale of the interchain coupling [17].

Magnetic fields applied within the ordering plane have a profoundly different effect from those along a. In fields along c a transition occurs above 1.4 T ($T < 0.3$ K) to a phase, marked S on Fig. 1(b), where (i) the structure is elliptical with a large elongation along the field direction, (ii) the incommensuration approaches a linear relation with field with a large slope [13] [see Fig. 1(e)], and (iii) the total ordered moment decreases with increasing field. Above 2.1 T there is no long-range order, at least down to 35 mK, and the system is in a spin liquid state. In this phase the dynamical correlations show shifts of continua and redistribution of scattering weight [10], as expected for spinon states and compared in [10] with 1D results [1]. However, 2D correlations are also important [by continuity they persist to the ferromagnetic F phase at saturation and to the spin liquid phase above T_N (both show 2D character)] and give rise to an asymmetric distribution of scattering weight at about $k = 1.5$ [10,13]. Linear field dependence of the incommensuration of the *longitudinal* spin correlations is a signature of exclusion statistics for the spinon quasiparticles in the HAFC, and the observed similar behavior of the incommensuration in the S phase dominated by the ordering of the *longitudinal* spin components suggests that *exclusion statistics are important for the quasiparticles in Cs_2CuCl_4*. The existence of a modulated continuum upper boundary indicating phase space restrictions for paired states also supports this conclusion. Susceptibility measurements [13] show no evidence of a phase transition between the spin liquid behavior in zero field above $T_N = 0.62$ K and the disordered phase found for fields greater than 2.1 T down to at least 35 mK. *This indicates that fields applied within the ordering plane stabilize the fractional spin liquid state*.

In conclusion we have studied the ground state and excitations of the frustrated quantum antiferromagnet Cs_2CuCl_4. This material has a 2D Hamiltonian interpolating between the square, triangular, and 1D Heisenberg antiferromagnets, and shows (i) very strong quantum renormalizations indicating the importance of fluctuations, (ii) continua in the dynamical correlations demonstrating fractional excitations, (iii) very large field-driven incommensuration and disorder effects from in-plane fields showing that exclusion statistics are important, and (iv) stabilization of a spin liquid ground state by in-plane fields. We believe new theoretical work is needed to explain these findings.

Full details of the analysis and extensive results from other related experiments on Cs_2CuCl_4 will be given in a forthcoming publication [13].

We thank M. Eskildsen, M. A. Adams and M. J. Bull for technical support and we acknowledge very useful discussions with D. F. McMorrow, R. A. Cowley, F. H. L. Essler, A. O. Gogolin, and M. Kenzelmann. ORNL is managed for the U.S. DOE by UT-Battelle, LLC, under Contract No. DE-AC05-00OR22725. A. M. T. is grateful to Isaac Newton Institute and Trinity College, Cambridge, for kind hospitality.

[1] G. Müller *et al.,* Phys. Rev. B **24**, 1429 (1981); J. C. Talstra and F. D. M. Haldane, Phys. Rev. B **50**, 6889 (1994).
[2] D. A. Tennant *et al.,* Phys. Rev. B **52**, 13 368 (1995); D. C. Dender *et al.,* Phys. Rev. B **53**, 2583 (1996).
[3] P. W. Anderson, Mater. Res. Bull. **8**, 153 (1973).
[4] V. Kalmeyer and R. B. Laughlin, Phys. Rev. Lett. **59**, 2095 (1987); Phys. Rev. B **39**, 11 879 (1989).
[5] L. B. Ioffe and A. I. Larkin, Phys. Rev. B **39**, 8988 (1989).
[6] P. A. Lee and N. Nagaosa, Phys. Rev. B **46**, 5621 (1992).
[7] S. M. Hayden *et al.,* Phys. Rev. Lett. **67**, 3622 (1991); S. J. Clarke *et al.,* Solid State Commun. **112**, 561 (1999).
[8] See, for example, S. Sachdev, in *Quantum Phase Transitions* (Cambridge University Press, Cambridge, UK, 1999), Chap. 13.
[9] S. Watanabe and H. Yokoyama, J. Phys. Soc. Jpn. **68**, 2073 (1999); D. Allen, F. H. L. Essler, and A. A. Nersesyan, Phys. Rev. B **61**, 8871 (2000); C. H. Chung, J. B. Marston, and R. H. McKenzie, cond-mat/0012216.
[10] R. Coldea *et al.,* Phys. Rev. Lett. **79**, 151 (1997).
[11] R. Coldea *et al.,* J. Phys. Condens. Matter **8**, 7473 (1996); J. Magn. Magn. Mater. **177**, 659 (1998).
[12] X.-G. Wen, F. Wilczek, and A. Zee, Phys. Rev. B **39**, 11 413 (1989); R. B. Laughlin, Science **242**, 525 (1988).
[13] R. Coldea *et al.* (to be published).
[14] Z. Weihong, R. H. McKenzie, and R. R. P. Singh, Phys. Rev. B **59**, 14 367 (1999).
[15] J. Jensen and A. R. Mackintosh, in *Rare Earth Magnetism. Structures and Excitations* (Clarendon, Oxford, 1991), p. 291.
[16] D. A. Tennant *et al.,* Phys. Rev. B **52**, 13 381 (1995).
[17] H. J. Schulz, Phys. Rev. Lett. **77**, 2790 (1996); F. H. L. Essler, A. M. Tsvelik, and G. Delfino, Phys. Rev. B **56**, 11001 (1997); B. Lake, D. A. Tennant, and S. E. Nagler, Phys. Rev. Lett. **85**, 832 (2000).